

Engineering of the qubit initialization in an imperfect physical system

Tianfeng Chen^{1,2}, Lin Wan^{1,2}, Jiamin Qiu^{1,2}, Hong Peng^{1,2}, Jie Lu^{3,4*}, and Ying Yan^{1,2*}

¹School of Optoelectronic Science and Engineering & Collaborative Innovation Center of Suzhou Nano Science and Technology, Soochow University, Suzhou 215006, China

²Key Lab of Advanced Optical Manufacturing Technologies of Jiangsu Province & Key Lab of Modern Optical Technologies of Education Ministry of China, Soochow University, 215006 Suzhou, China

³Department of Physics, Shanghai University, 200444 Shanghai, China

⁴Shanghai Key Lab for Astrophysics, 100 Guilin Road, 200234 Shanghai, China

* Corresponding authors: lujie@shu.edu.cn (J. Lu); yingyan@suda.edu.cn (Y. Yan).

Abstract

We proposed a method to engineer the light matter interaction while initializing a qubit in presence of physical constraints utilizing the inverse engineering. Combining the multiple degrees of freedom in the pulse parameters with the perturbation theory, we developed pulses to initialize the qubit within a tightly packed frequency interval to an arbitrary superposition state with high fidelity. Importantly, the initialization induces low off-resonant excitations to the neighboring qubits, and it is robust against the spatial inhomogeneity in the laser intensity. We applied the method to the ensemble rare-earth ions system, and simulations show that the initialization is more robust against the variations in laser intensity than the previous pulses, and reduces the time that ions spend in the intermediate excited state by a factor of 17. The method is applicable to any systems addressed in frequency such as NV centers, superconducting qubits, quantum dots, and molecular qubit systems.

Keywords: qubit initialization; robust operation; frequency detuning; off-resonant excitation; spatial inhomogeneity in laser intensity

Introduction

High precision coherent control of quantum systems is essential to the state initialization and manipulation in quantum computing [1], quantum communications [2, 3], quantum simulation [4], and quantum metrology [5]. Among any complicated coherent controls for qubits, the startup step is the same, i.e. initializing a qubit to an arbitrary superposition state in fast timescale and with high fidelity. It is a challenging task to achieve the high-fidelity initialization in some imperfect experimental systems, where unavoidable physical constraints are in presence. For example, the addressing frequency of an ensemble qubit in the rare-earth ions (REI) qubit system inhomogeneously spreads within a few hundred kHz [6, 7]. High fidelity manipulation on this ensemble qubit demands a uniform coherent control over this tightly-packed frequency interval [8, 9]. Another constraint impeding the high-fidelity control is the unwanted off-resonant excitations, typically lying about a few MHz away from the qubit frequency, originating from other transitions of the neighboring qubits closely spaced in frequency [10-12]. Besides these two constraints, another restriction in experiments which degrades the fidelity is the uneven spatial distribution of the laser intensity under detection. In most cases a plane wave with constant intensity is considered in theoretical works, which is true only for the very center part of a Gaussian beam. For this, one can use a pinhole in the detection system to intentionally select the center part of the beam for detection, but pays the price by the huge drop in the signal strength, which results in a low signal to noise ratio, therefore affects the accuracy of the measurements. High fidelity initialization on a qubit in such an imperfect system would require that the quantum control simultaneously overcome

all these three constraints. Firstly, it is robust against the frequency detuning within a tightly packed frequency interval. Secondly, it causes negligible unwanted off-resonant excitations to the qubits close by in frequency. Thirdly, it is robust against the inhomogeneous variations in the laser intensity, or equivalently in the Rabi frequency. Our work aims for designing fast and robust pulses which are capable of initializing a qubit in such an imperfect physical system to an arbitrary superposition state.

Adiabatic passage (STIRAP and their variants) is widely used [13-16] to improve the robustness of the quantum control against the frequency detuning, variation in pulse area, and timing errors. However, the state evolution is slow limited by the adiabatic theorem, which potentially increases the decoherence. Combining fast speed with high robustness, shortcuts to adiabaticity (STA) was proposed [17-20]. STA provides a nonadiabatic route towards the results which the adiabatic passage can achieve, where several techniques were investigated: inverse engineering based on the Lewis-Riesenfeld (LR) invariant [21-24], counter diabatic driving [17, 25], and fast-forward approach [26]. Each technique has different characteristics and may apply to different experimental systems [24]. Inverse engineering offers more flexibility to design the exact dynamical evolution while ensuring the target states via boundary conditions. It has been used to develop pulses which has high robustness against the variations in frequency, and at the same time causes negligible off-resonant excitations by optimizing the multiple degrees of freedom introduced in the pulse parameters [10]. However, to demonstrate the high-fidelity manipulation in experiments, a pinhole is needed in the detection system to intentionally select the most central part of the Gaussian beam where Rabi frequency varies less than 5% [27]. In this work we treated the variation in Rabi frequency as a perturbation, employed the perturbation theory to investigate the reduction in fidelity, and developed pulses which simultaneously overcome all three aforementioned constraints. We applied the method to the REI system, which is an ideal system to verify the constraints of both the frequency inhomogeneity and unwanted off-resonant excitations. Importantly, REI system is an excellent test bed for both quantum computation and quantum memory because of their long coherence properties [28]. A comparison with the pulses developed previously shows that the pulses in this work has better performance with respect to the Rabi frequency variations. The method is applicable to any imperfect systems addressed in frequency such as NV centers [29], superconducting qubits [11], quantum dots [30], and molecular qubit systems [12].

The article is arranged as follows. We first introduce the inverse engineering scheme in a three-level system and the systemic error sensitivity in the frame of perturbation theory. Then we propose a method to construct the fast, robust, and low off-resonant excitation pulses, and show the performance of the pulses in simulation in application to the REI system. In the end we discuss the results and present the conclusion.

Invariant-based inverse engineering and systematic error sensitivity

Under the rotating wave approximation, the Hamiltonian of a three-level system as shown in Fig. 1, reads [31]

$$H_0(t) = \frac{\hbar}{2} \begin{bmatrix} 0 & \Omega_p(t) & 0 \\ \Omega_p(t) & 0 & \Omega_s(t)e^{-i\varphi} \\ 0 & \Omega_s(t)e^{i\varphi} & 0 \end{bmatrix}, \quad (1)$$

where $\Omega_{s,p}$ is the Rabi frequency describing the coupling between light pulses and atomic transitions, $\Omega_i = -\frac{\vec{\mu}_i \cdot \vec{E}_i}{\hbar}$ ($i = s, p$), $\vec{\mu}_i$ denotes the transition dipole moments, \vec{E}_i the electric field, and φ a time-independent phase of the field Ω_s . L-R theory tells that the eigenstates of the L-R invariants of the time-dependent Hamiltonian can be used to construct the states of the system driven by that Hamiltonian.

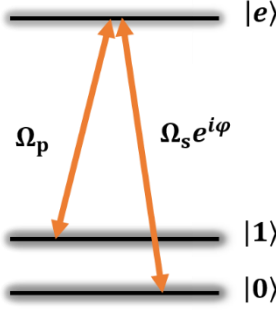


Fig. 1. (Color online) Schematic energy-level diagram in a Λ configuration. The qubit is presented by level $|0\rangle$ and $|1\rangle$, which are coupled by the optical transitions $|1\rangle - |e\rangle$ and $|0\rangle - |e\rangle$ with driving fields Ω_p and $\Omega_s e^{i\varphi}$, respectively, where φ is a time-independent phase.

The L-R invariant $I(t)$ of the Hamiltonian $H_0(t)$, satisfying $i\hbar \frac{\partial I(t)}{\partial t} - [H_0(t), I(t)] = 0$, is

$$I(t) = \frac{\hbar\Omega_0}{2} \begin{bmatrix} 0 & \cos\gamma(t)\sin\beta(t) & -i\sin\gamma(t)e^{-i\varphi} \\ \cos\gamma(t)\sin\beta(t) & 0 & \cos\gamma(t)\cos\beta(t)e^{-i\varphi} \\ i\sin\gamma(t)e^{i\varphi} & \cos\gamma(t)\cos\beta(t)e^{i\varphi} & 0 \end{bmatrix}, \quad (2)$$

where Ω_0 is a constant in unit of frequency, and $\gamma(t)$ and $\beta(t)$ are time-dependent parameters to be determined [10]. The invariant $I(t)$ has three eigenstates $|\phi_0(t)\rangle$ and $|\phi_{\pm}(t)\rangle$ with eigenvalues λ_0 and λ_{\pm} , and the corresponding L-R phases are α_0 and α_{\pm} . The L-R theory shows that the superposition of these eigenstates multiplied by the respective L-R phases is a solution of the Schrödinger equation with the Hamiltonian $H_0(t)$ [24]. In this work we are interested in the eigenstate

$$|\phi_0(t)\rangle = \begin{bmatrix} \cos\gamma(t)\cos\beta(t) \\ -i\sin\gamma(t) \\ -\cos\gamma(t)\sin\beta(t)e^{i\varphi} \end{bmatrix}, \quad (3)$$

with eigenvalue $\lambda_0 = 0$ and L-R phase $\alpha_0 = 0$. It is easy to check that $|\phi_0(t)\rangle$ itself satisfies the Schrödinger equation. Thus, the system Hamiltonian $H_0(t)$ can drive the qubit state evolving along the state $|\phi_0(t)\rangle$. This knowledge on the state evolution provides us the convenience of ensuring the initial and final state as we wish, in the meanwhile maintaining the freedom to design the specific evolution path governed by the exact form of $\gamma(t)$ and $\beta(t)$.

The Rabi frequency Ω_i ($i = s, p$) in $H_0(t)$ relates to $\gamma(t)$ and $\beta(t)$ in the invariant $I(t)$, as follows

$$\Omega_p = 2[\dot{\beta}\cot\gamma(t)\sin\beta(t) + \dot{\gamma}\cos\beta(t)], \quad (4)$$

$$\Omega_s = 2[\dot{\beta}\cot\gamma(t)\cos\beta(t) - \dot{\gamma}\sin\beta(t)]. \quad (5)$$

Eqs. (4) and (5) tells that once the time-dependent $\gamma(t)$ and $\beta(t)$ are designed, the Rabi frequencies Ω_i are known. As an illustration, we consider the Hamiltonian in Eq. (1) drives the qubit state from the initial state $|1\rangle$ to a target state $|\psi_{target}\rangle = \cos\theta|1\rangle + \sin\theta e^{i\varphi}|0\rangle$ (θ and φ are arbitrary angles), along the eigenstate $|\phi_0(t)\rangle$ within an operation time of t_f . This implies that $|\phi_0(0)\rangle = |1\rangle$ and $|\phi_0(t_f)\rangle = |\psi_{target}\rangle$, which impose boundary conditions to $\gamma(t)$ and $\beta(t)$. However, the exact ansatzs of $\gamma(t)$ and $\beta(t)$ are still free to design as long as they meet the boundary conditions. This freedom might be used for optimizing the performance of the light pulses, such as achieving a robust quantum control against frequency detuning, and the variations in laser intensity.

The variation in laser intensity is regarded as a perturbation to the system Hamiltonian $H_0(t)$, and its effect is treated in perturbation theory. Considering the variation in laser intensity, the total Hamiltonian of the system is

$$H = H_0 + H_1, \quad (6)$$

where $H_1 = \lambda H_0$, and $\lambda \in [0,1]$ represents the strength of the perturbing Hamiltonian resulted from the laser intensity variation. The fidelity of achieving the target states in this case is $P = \left| \langle \psi_{target} | \psi'_{t_f} \rangle \right|^2 = 1 - \lambda^2 \left| \int_0^{t_f} e^{-i\alpha_+(t)} (\dot{\beta} \cos \gamma + i \dot{\gamma}) dt \right|^2$, where $|\psi'_{t_f}\rangle$ is the final state attained with the perturbation theory. To investigate the sensitivity of P on λ , the systematic error sensitivity is used [32], which reads

$$q_s = -\frac{1}{2} \frac{\partial^2 P}{\partial \lambda^2} \Big|_{\lambda=0} = \left| \int_0^{t_f} e^{-i\alpha_+(t)} (\dot{\beta} \cos \gamma + i \dot{\gamma}) dt \right|^2, \quad (7)$$

where $\alpha_+(t) = - \int_0^t \frac{\dot{\beta}(t')}{\sin \gamma(t')} dt'$. The closer q_s approaches to zero, the more robust the quantum control is against variations in laser intensity.

In what follows, we will develop the light pulses by proposing the exact ansatz of $\gamma(t)$ and $\beta(t)$ that satisfy the boundary conditions on $|\phi_0(0)\rangle$ and $|\phi_0(t_f)\rangle$, in the meanwhile ensure $q_s \approx 0$ to guarantee the insensitivity of the quantum control in respect to the variations in laser intensity.

Model and the simulation results

The boundary conditions of $\gamma(t)$ and $\beta(t)$ restricted by $|\phi_0(0)\rangle = |1\rangle$ and $|\phi_0(t_f)\rangle = |\psi_{target}\rangle$ are

$$\gamma(0) = \gamma(t_f) = \pi, \quad (8)$$

$$\beta(0) = \pi, \beta(t_f) = \pi - \theta. \quad (9)$$

In addition, considering the requirements on error sensitivity $q_s \approx 0$, we propose the ansatz of $\gamma(t)$, $\beta(t)$ as follows

$$\gamma(t) = \pi + \sum_{m=1}^{\infty} A_m e^{-\frac{(t-B_m t_f)^2}{(C_m t_f)^2}}, \quad (10)$$

$$\beta(t) = -\frac{\theta_a}{t_f} t + \frac{\theta_a}{\pi} \sum_{n=1}^{\infty} a_n \sin\left(\frac{n\pi t}{t_f}\right) + \pi. \quad (11)$$

where A_m , B_m , and C_m denotes the amplitude, center position, and the width of each Gaussian component, respectively. They have to be carefully adjusted so that the Gaussian components contribute to $\gamma(t)$ at the starting and ending time only by an infinitesimal constant ε . a_n in Eq. (11) denotes the amplitude of each sinusoidal component, and is independent on the boundary values of $\beta(t)$.

Besides the limitation of boundary conditions and error sensitivity, Rabi frequencies are preferred to start from and end with zero in most experimental implementations, to avoid sharp changes in light intensity. The reason is that the redundant frequency components within the sharp changes could disturb the qubit operation. This demands that

$$\Omega_s(t=0, t_f) = \Omega_p(t=0, t_f) = 0. \quad (12)$$

For this, a_n , A_m , B_m and C_m have to satisfy

$$a_1 + 3a_3 + 5a_5 + 7a_7 + \dots = 0, \quad (13)$$

$$a_2 + 2a_4 + 3a_6 + 4a_8 + \dots = 0.5, \quad (14)$$

$$\sum_{m=1}^{\infty} A_m \cdot \frac{2(t - B_m t_f)}{C_m^2 t_f} e^{-\frac{(t - B_m t_f)^2}{(C_m t_f)^2}} \Big|_{t=0, t_f} \approx 0. \quad (15)$$

In the following passage, we will apply the pulse-designing protocol shown above in the ensemble REI qubit system to illustrate how to tailor the pulses to achieve the robust quantum operations through optimizing the multiple degrees of freedom in a_n . High fidelity operation in this system requires that the pulses not only interact with the ensemble qubit ions as efficient as possible regardless of the ± 170 kHz frequency detuning between them, but also address the neighboring ions which is about ± 3.5 MHz away from the qubit ions as little as possible, to suppress the off-resonant excitations. Performance of the pulses is evaluated by the operational fidelity as

$$F = \left| \langle \psi_{target} | \psi_{t_f} \rangle \right|^2, \quad (16)$$

where $|\psi_{t_f}\rangle = [C_1(t_f), C_e(t_f), C_0(t_f)]^T$ is the final state of the quantum system driven by the Hamiltonian H_0 [10], and $C_n (n = 1, e, 0)$ is the probability amplitude being on level $|1\rangle$, $|e\rangle$, $|0\rangle$, respectively.

Taking $|\psi_{target}\rangle = \frac{1}{\sqrt{2}}(|1\rangle + i|0\rangle)$ ($\theta = \frac{\pi}{4}$, $\varphi = \frac{\pi}{2}$) and $t_f = 4 \mu s$ as an example, we found that the pulses with parameters A_m , B_m , C_m , and a_n as shown in Table 1 could create the target state in high fidelity and with high robustness against the frequency detuning and intensity variations within the qubit ions, in the meanwhile induce low off-resonant excitations to the nearby ions closely spaced in frequency. The procedures to look for the Gaussian-related parameters (A_m , B_m , C_m) are shown in the Appendix, and the optimization of a_n is done by using the *fgoalattain* in MATLAB at given values of the Gaussian parameters. For simplicity but without losing generality, $m = 3$ and $n = 8$ are considered in this work. The error sensitivity in laser intensity of these pulses is $q_s = 0.0137$.

Table 1. Parameters of Gaussian terms in Eq. (10) and Optimal a_n values of $\beta(t)$ in Eq. (11)

	The first Gaussian	The second Gaussian	The third Gaussian
Weight factor A_m	0.08	0.04	0.03
Pulse center B_m	0.5	0.5	0.5
Pulse width C_m	0.4	0.31	0.28
with the A_m , B_m , and C_m given above, the optimized a_n parameters are as follows			
a_1	a_2	a_3	a_4
0.36	0.8378	0.04	-0.0329
a_5	a_6	a_7	a_8
-0.02	-0.0639	-0.0543	-0.0201

The time evolution of Rabi frequencies $\Omega_{s,p}$ and the qubit state are depicted in Fig. 2(a) and Fig. 2(b), respectively. All population starts from the ground state $|1\rangle$ and ends with an equal distribution on $|1\rangle$ and $|0\rangle$ as expected. The small deviation from 50% at time t_f results from the excitation by the tail of the Gaussian functions in $\gamma(t)$. Within the operation, the excited state $|e\rangle$ is hardly populated, and the time that ions spend in the excited state is only $0.04 \mu s$. It is 17 times shorter than that in the previous work [10], which strongly decreases the possibility of spontaneous decay, and ensure a higher operational fidelity.

The pulses shown above can perform robust quantum control in high fidelity over the ensemble qubit in despite of the frequency detuning and variations in laser intensity. Moreover, the pulses induce low off-resonant excitations to the ions closely spaced in frequency with the qubit of interest.

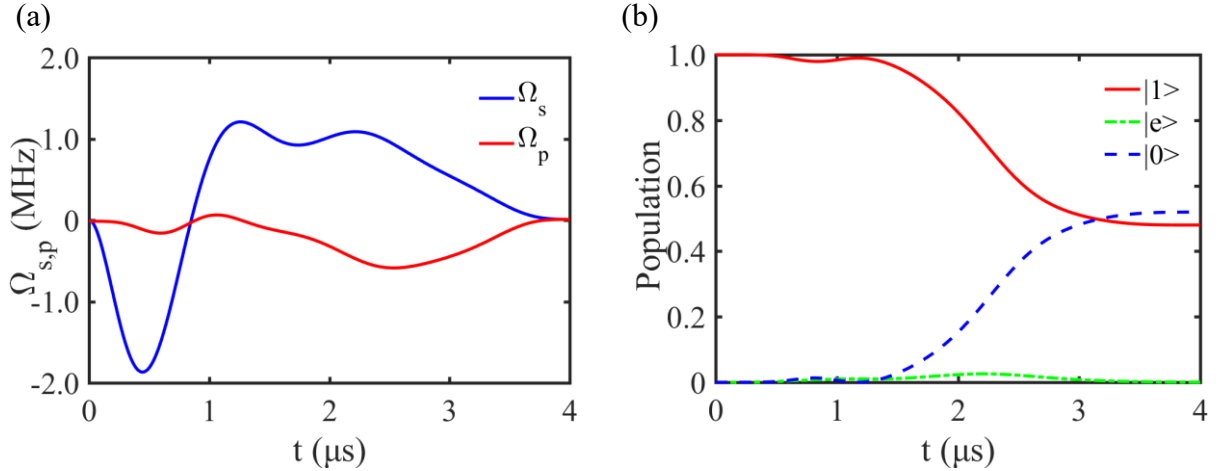


Fig. 2. (Color online) (a) Rabi frequency Ω_s (blue) and Ω_p (red) of the pulses in this work. (b) Time evolution of the qubit state in level $|1\rangle$ (solid red), $|e\rangle$ (dash-dotted green), and $|0\rangle$ (dashed blue). The initial state is $|1\rangle$ and the target state is $|\psi_{target}\rangle = \frac{1}{\sqrt{2}}(|1\rangle + i|0\rangle)$.

A. Robustness to frequency detuning and suppression of off-resonant excitations

The dependence of the fidelity F on the frequency detuning is shown in Fig. 3. The fidelity is more than 99.7% within the frequency detuning ranges of ± 270 kHz (see the inset) which indicates that the pulses can interact with all ions within this frequency span equally good. The fidelity outside the range of ± 3.5 MHz remains around 50% which is accounted for by the overlap between the initial states ($|1\rangle$) and the target state.

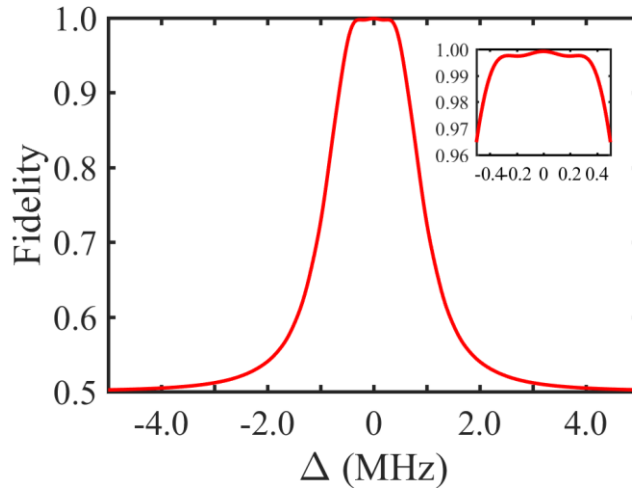


Fig. 3. (Color online) Dependence of the operational fidelity on the frequency detuning, where the qubit is initially in state $|1\rangle$, and the target state is $|\psi_{target}\rangle = \frac{1}{\sqrt{2}}(|1\rangle + i|0\rangle)$.

The off-resonant excitation of the neighboring ions which are closely spaced in frequency to the qubit ions were investigated by the dependence of population in level $|1\rangle$, $|e\rangle$ and $|0\rangle$ on frequency detuning, as shown in Fig. 4. Within ± 270 kHz around the center frequency, the population on level $|0\rangle$ and $|1\rangle$ fluctuates around 50%. Outside ± 3.5 MHz, 94.2% population is on $|1\rangle$ state, which means that the off-resonant excitation is about 5.8%. It may be

accepted because the ion density within this range is much less than that in the center. Furthermore, it might be reduced by sacrificing the robust region in the center via adjusting the Gaussian parameters and values of a_n . In addition, the ± 3.5 MHz turning point could be pushed further away from the center if Eu ions with larger energy level separations were used instead of Pr ions [33].

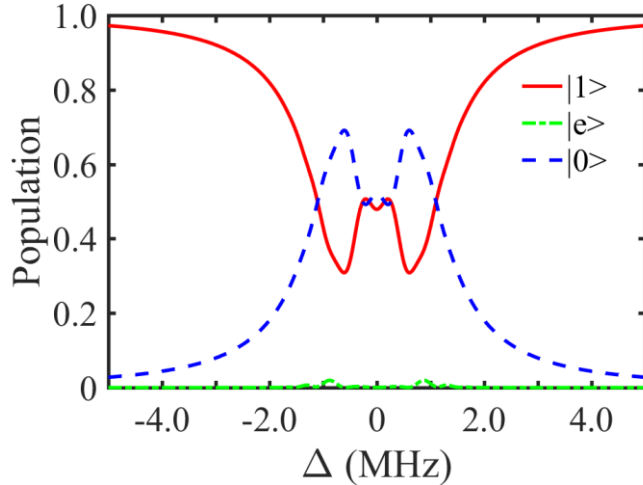


Fig. 4. (Color online) Dependence of the population of the final state in level $|1\rangle$ (solid-red), $|e\rangle$ (dash-dotted green) and $|0\rangle$ (dashed blue) on the frequency detuning.

B. Robustness to variations in laser intensity

In experiments, a Gaussian beam is widely used where the laser intensity varies with the distance to the center of the beam. This spatial inhomogeneity results in different operational fidelity at different spatial locations within the laser focus. For detecting the high-fidelity operation, a pinhole is normally used in the detection system to intentionally select the most center part of the focus, where the intensity variation is negligible, in the price of lowering down the detection signal and further the signal to noise ratio (SNR). The pulses developed in this work is robust against the variation in light intensity, potentially reducing the necessity to use a pinhole and increasing the SNR.

The dependence of fidelity on the variations in the Rabi frequency at different detuning frequencies using the pulses in Fig. 2(a) is shown in Fig. 5(a), where $\eta = \delta\Omega_{p,s}/\Omega_{p,s}$ represents the fractional variation in Rabi frequency, and Δ denotes the frequency detuning. In case of no detuning, the fidelity is above 97% over $\pm 30\%$ variation in the Rabi frequency. In presence of detuning, the pulses are more robust against the positive variations than the negative ones. As a comparison, the same investigation using the pulses proposed in article [24] was done. The results are shown in Fig. 5(b), where the robust range is smaller, attributed to the non-zero error sensitivity ($q_s = 0.5847$ at $\Delta = 0$). It is 43 times larger than our pulses.

The effective fidelity, \bar{F} , achieved with a Gaussian beam with a focal radius of r was investigated. The result is shown in Fig. 6, where the r/w_0 denotes the radius of the beam with respect to its waist w_0 at $1/e^2$. \bar{F} is defined as follows

$$\bar{F} = \sum_{i=1}^N p(r_i) \cdot F(r_i), \quad (16)$$

where $p(r_i) = \frac{\int_{r_{i-1}}^{r_i} \Omega(r) dr}{\int_0^T \Omega(r) dr}$ ($1 \leq i \leq N, r_i = \frac{i}{N} r$) represents the weight of the fidelity $F(r_i)$ in the ring with radius from r_{i-1} to r_i . The solid-red line (dashed-red) shows the dependence of \bar{F} on the beam radius using the pulses

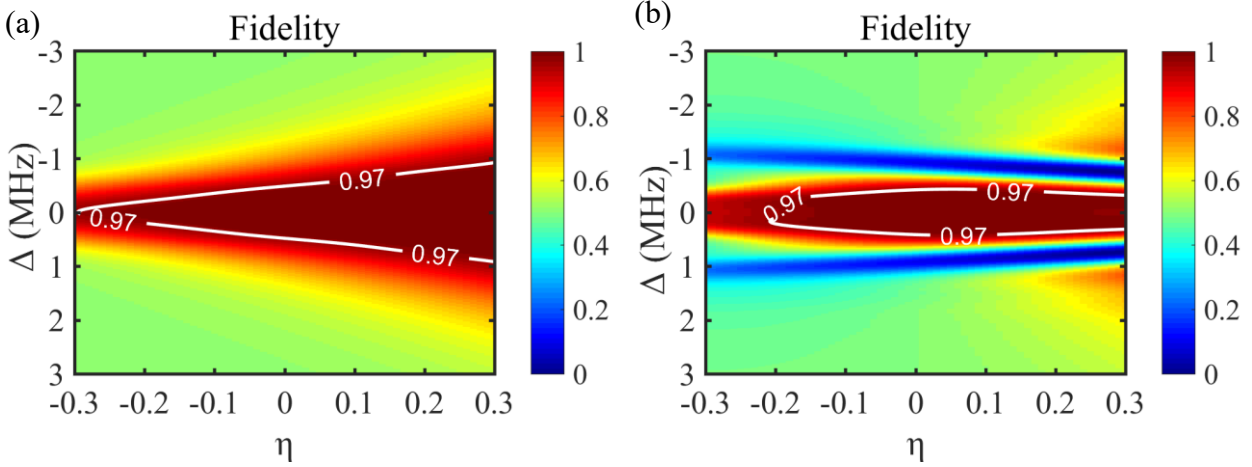


Fig. 5. (Color online) Dependence of the fidelity on the variation in Rabi frequency at different frequency detuning. (a): using the pulses in this work. (b): using the pulses in the article [24]. η denotes the fractional variation in Rabi frequency, and Δ denotes the frequency detuning.

shown in this work (in Ref. [10]) at zero detuning. The effective fidelity reaches 93% using our pulses if the signal is collected from a beam with diameter of $2w_0$, while it is only about 88% using the previous pulses. It is clear that the pulses in this work are more robust against the inhomogeneity in the light intensity benefiting from the perturbation theory. The inset shows the results using both types of pulses where the frequency detuning is not zero but 170 kHz. There the difference is not significant, because the perturbation theory in our framework only applies to the on-resonance interaction. The actual fidelity one would expect in experiments is a weighted combination of the red and blue curve depending on the exact profile of the absorption peaks representing the qubit.

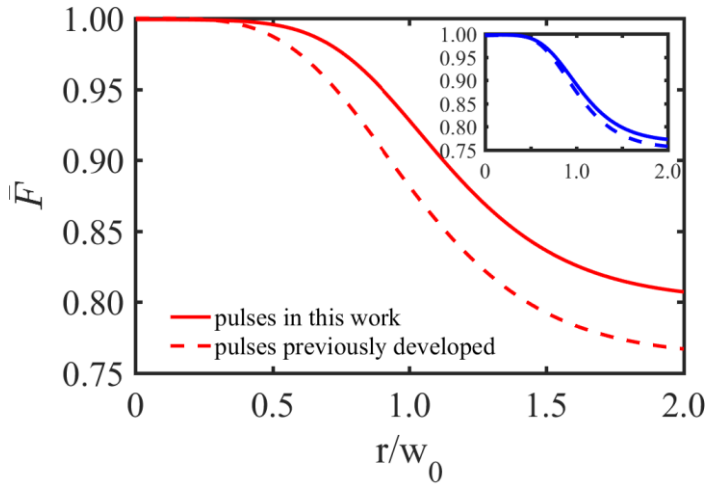


Fig. 6. (Color online) The effective fidelity achieved with a Gaussian beam with a focal radius of r under detection by using our pulses (solid lines) and the pulses reported in Ref. [10] (dashed lines). Red lines: on resonance. Blue lines: with a frequency detuning of 170 kHz. w_0 represents the beam waist.

C. Dependence of the off-resonant excitations and operation fidelity on the variation in a_n

In practice, light pulses experimentally generated may deviate from the optimal waveform defined by the

parameters shown in Table 1 limited by the electronic noises, instrumental accuracy, or variation in temperature of the waveform generators. Thus, it is interesting to investigate the dependence of the pulse performance on the variation in these parameters. As a qualitative yet instructive illustration, we considered the variation in a_2 since it has the largest weight among all the parameters. The results are shown in Fig. 8(a) and 8(b), where $\delta = \Delta a_2 / a_2$ is the fractional variation of a_2 , Δ is the frequency detuning, and P_0 denotes the population in level $|0\rangle$. Ideally, one would expect the ions which are ± 3.5 MHz away from the qubit are untouched by the pulses, that is, they remain in their initial state of $|1\rangle$. Thus $P_0 \approx 0$, as shown by Fig. 8(a), where only the positive axis of the detuning is plotted as the dependence is symmetric. The off-resonant excitations increase gradually with the increasing variation in δ .

The operational fidelity is quite robust against the variation in δ within the frequency detuning range of ± 270 kHz. The reason for this is that the population in level $|e\rangle$ hardly changes with the fluctuations in a_2 , keeping on nearly zero. Thus, the fidelity can be simplified as $F = 0.5 + \text{Im}(C_1^* C_0)$, where the imaginary part $\text{Im}(C_1^* C_0)$ depends on the variation in δ weakly.

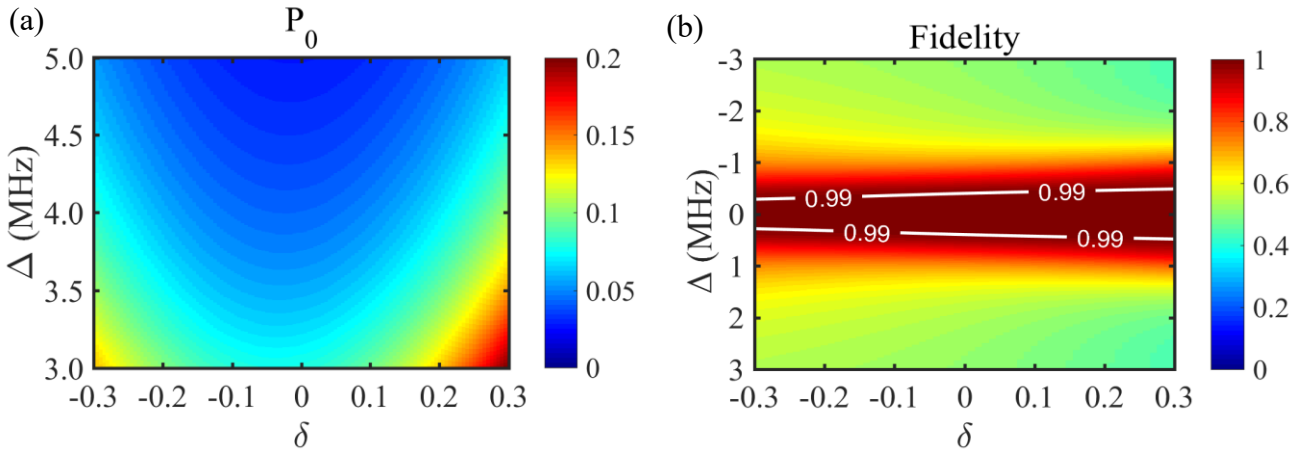


Fig.7. (Color online) Influence of the fractional variation δ in a_2 on (a) the off-resonant excitation and (b) the fidelity at different frequency detuning.

Above pulses are physically feasible. The magnitude of the Rabi frequency is less than 2 MHz, which can be easily achieved in the laboratory. The time-dependence profile can be initially generated by an arbitrary waveform generator as an electronic radio-frequency (RF) signal, then the RF signal drives an acousto-optical modulator to create the light pulses through the first order deflection.

Discussion and conclusion

We have proposed a method to develop robust pulses for creating an arbitrary superposition qubit state in an imperfect three-level system with high fidelity by using the invariant-based inverse engineering combined with the perturbation theory. The light pulses are built from multiple Gaussian and sinusoidal components. The multiple degrees of freedom in the Gaussian and sinusoidal terms provides us the opportunity to tailor the pulse performance in respect to the constraints present in the quantum system. We applied this method in the REI system, and the simulation shows that our pulses are able to create a superposition state with fidelity more than 99.7% over a frequency detuning range of ± 270 kHz in an operation time of 4 μ s, and the off-resonant excitation of the ions close by in frequency is below 5.8%, in the mean while the operation is more robust against the inhomogeneous distribution in the light intensity than the previous nonadiabatic pulses [10]. More importantly, the time that ions spend in the excited state is only about one percent of the operation time and 17 times shorter than that presented in the previous work [10]. This potentially decreases the effect of decoherence, ensuring a higher fidelity. We need to say that the

error sensitivity caused by the inhomogeneity in Rabi frequency was investigated in the frame work of no frequency detuning at presence. If the detuning is considered as well in the perturbation theory, the robustness against this inhomogeneity may be further improved, which lies out of the scope of this work.

The pulse-designing protocol shown in this work applies to any imperfect quantum system where qubits are closely spaced in frequency including but not limited to the REI qubit system, superconducting qubits, and the molecular qubit system. Though the protocol is introduced in a three-level system, it can be used for population transfers in a simple two-level system if just one light field is used.

Appendix

Here we provide a guide for choosing the appropriate values of the parameters in the Gaussian functions shown in $\gamma(t)$ as shown in Eq. (10).

Each Gaussian term in Eq. (10) are determined by three parameters, A_m , B_m , and C_m , which specify the amplitude, center position, and the width, respectively. Appropriate values need to be taken to ensure that the quantum control works as we expect.

There are two restrictions to the value of A_m . First, $A_m \neq 0$ so that the Gaussian terms contribute to suppress the off-resonant excitations caused by the sinusoidal terms in Eq. (11). Second, A_m should be small enough so that $\gamma(t)$ deviates from π by a small constant ε . With this, the error sensitivity q_s is as follows

$$q_s = \left| (-i) \cdot \varepsilon \cdot \left(e^{i \frac{6\theta_a}{6\varepsilon - \varepsilon^3}} - 1 \right) \right|^2 \quad (17)$$

where $q_s \in [0, 4\varepsilon^2]$. Clearly, q_s approaches zero as ε gets smaller. Therefore, robustness against the variations in Rabi frequency can be achieved.

For B_m , Eq. (15) needs to be evaluated, which is as follows at $t = 0$ and $t = t_f$, respectively

$$\sum_{m=1}^{\infty} A_m \frac{2(-B_m)}{C_m^2} e^{-\left(\frac{B_m}{C_m}\right)^2} = 0, \quad (18)$$

$$\sum_{m=1}^{\infty} A_m \frac{2(1-B_m)}{C_m^2} e^{-\left(\frac{1-B_m}{C_m}\right)^2} = 0 \quad (19)$$

Obviously, the best choice for B_m is 0.5 so that the two equations reduce to a single one.

The effect of C_m is not as transparent as that for A_m and B_m . To investigate this, we set $A_1 = 0.1$, $B_1 = 0.5$, $a_2 = 0.5$, and all other A_m , B_m , C_m ($m \neq 1$) and a_n ($n \neq 2$) are zeros, and check how the operation fidelity changes in response to different values of C_1 . The results are shown in Fig. 8. We found that a wider Gaussian pulse results in a narrower response in fidelity to the frequency detuning. This makes sense seen from the Fourier transform perspective. However, C_1 can't be too large, otherwise the boundary values of $\gamma(t)$ will deviate from its expected value of π too much. This will eventually degrade the operational fidelity.

With all above considerations in mind, we set the A_m , B_m , and C_m values as shown in Table 1, and did an optimization on a_n in $\beta(t)$, and developed the pulses with desired performance as shown in the main text. It is worth to note that the values given in this work are just one option. Other alternatives potentially could provide the same performance.

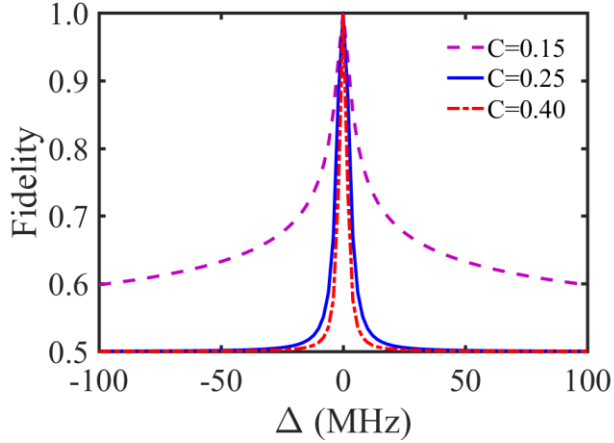


Fig. 8. (Color online) Influence of C_1 of the single Gaussian term in $\gamma(t)$ on the fidelity. In this figure, $A_1 = 0.1$, $B_1 = 0.5$, $a_2 = 0.5$, and all the other parameters in $\gamma(t)$ and $\beta(t)$ are zeros.

Acknowledgement

The work was supported by National Natural Science Foundation of China (NSFC) (61505133, 61674112, 62074107); Natural Science Foundation of JiangSu Province (BK20150308); The International Cooperation and Exchange of the National Natural Science Foundation of China NSFC-STINT (61811530020).

References

- [1] K. Hammerer, A. S. Sørensen, E. S. Polzik, Rev. Mod. Phys. 82 (2010)1041.
- [2] R. Horodecki, P. Horodecki, M. Horodecki, K. Horodecki, Rev. Mod. Phys. 81 (2009) 865.
- [3] N. Gisin, G. Ribordy, W. Tittel, Hugo Zbinden, Rev. Mod. Phys. 74 (2002) 145-195.
- [4] I. M. Georgescu, S. Ashhab, and F. Nori, Rev. Mod. Phys. 86 (2014) 153.
- [5] V. Giovannetti, Seth Lloyd, L. Maccone, Nat. Photonics 5 (2011) 222-229.
- [6] L. Rippe, M. Nilsson, S. Kröll, Phys. Rev. A 71 (2005) 062328.
- [7] L. Rippe, B. Julsgaard, A. Walther, Y. Ying, S. Kröll, Phys. Rev. A 77 (2008) 022307.
- [8] L. Wan, J. Moser, Y. Yan, Proc. of SPIE. 11339 (2019) 113390D-1.
- [9] Y. Yan, J. Lu, L. Wan, J. Moser, Phys. Lett. A 383, 600 (2019).
- [10] Y. Yan, Y.C. Li, A. Kinos, A. Walther, Opt. Express 27 (2019) 8267.
- [11] Y. Makhlin, G. Schöen, A. Shnirman, Rev. Mod. Phys. 73 (2001) 357.
- [12] K.K. Ni, T. Rosenband, D. D. Grimes, Chem. Sci. 9 (2018) 6830.
- [13] N.V. Vitanov, T. Halfmann, B.W. Shore, K. Bergmann, Annu. Rev. Phys. Chem. 52 (2001) 763.
- [14] P. Král, I. Thanopulos, M. Shapiro, Rev. Mod. Phys. 79 (2007) 53.
- [15] J.R. Kuklinski, U. Gaubatz, F.T. Hioe, K. Bergmann, Phys. Rev. A 40 (1989) 6741.
- [16] N. Sangouard, S. Guérin, L.P. Yatsenko, T. Halfmann, Phys. Rev. A 70 (2004) 013415.
- [17] X. Chen, I. Lizuain, A. Ruschhaupt, D. Guéry-Odelin, J.G. Muga, Phys. Rev. Lett. 105 (2010) 123003.
- [18] X. Chen, A. Ruschhaupt, S. Schmidt, A. del Campo, D. Guéry-Odelin, J.G. Muga, Phys. Rev. Lett. 104 (2010) 025009.
- [19] A. Baksic, H. Ribeiro, A.A. Clerk, Phys. Rev. Lett. 116 (2016) 230503.
- [20] H.L. Mortensen, J.J.W.H. Sørensen, K. Mølmer, aJ.F. Sherson, New J. Phys. 20 (2018) 025009.
- [21] A. Kiely, A. Ruschhaupt, J. Phys. B 47 (2014) 115501.
- [22] X. Chen, J.G. Muga, Phys. Rev. A 86 (2012) 033405.

- [23] H.R. Lewis, W.B. Riesenfeld, *J. Math. Phys.* 10 (1969) 1458.
- [24] X. Chen, E. Torrontegui, J.G. Muga, *Phys. Rev. Lett.* 83 (2011) 062116.
- [25] M.V. Berry, *J. Phys. A: Math. Theor.* 42 (2009) 365303.
- [26] S. Masuda, K. Nakamura, *Phys. Rev. A* 78 (2008) 062108.
- [27] The manuscript on the experimental work is in preparation.
- [28] M. Zhong, M.P. Hedges, R.L. Ahlefeldt, J.G. Bartholomew, S.E. Beavan, S.M. Witting, J.J. Longdell, M.J. Sellars, *Nature* 517 (2015) 177.
- [29] T. Nöbauer, A. Angerer, *Phys. Rev. Lett.* 115 (2015) 190801.
- [30] Y. Ban, X. Chen, E.Y. Sherman, aJ.G. Muga, *Phys. Rev. Lett.* 109 (2012) 206602.
- [31] K. Bergmann, H. Theuer, B.W. Shore, *Rev. Mod. Phys.* 70 (1998) 1003.
- [32] A. Ruschhaupt, X. Chen, D. Alonso, J.G. Muga, *New J. Phys.* 14 (2012) 093040.
- [33] R. W. Equall, Y. Sun, R. L. Cone, R. M. Macfarlane, *Phys. Rev. Lett.* 72 (1994) 2179.